PERIÓDICO TCHÊ QUÍMICA
ARTIGO ORIGINAL

AVALIAÇÃO DOS PARÂMETROS DA SUPERFÍCIE DE CONTATO NA SUPERFÍCIE DE TROCADOR DE CALOR COM ALETAS SERRILHADAS POR SERRILHAS EM AROS VAZIOS

EVALUATION OF THE CONTACT SURFACE PARAMETERS AT KNURLING FINNED HEAT-EXCHANGING SURFACE BY KNURLS AT RING BLANKS

ОЦЕНКА ПАРАМЕТРОВ КОНТАКТНОЙ ПОВЕРХНОСТИ ПРИ НАКАТЫВАНИИ ОРЕБРЕННОЙ ТЕПЛООБМЕННОЙ ПОВЕРХНОСТИ РОЛИКАМИ НА КОЛЬЦЕВЫХ ЗАГОТОВКАХ

TATARKANOV, Aslan Adal`bievich[1]; ALEXANDROV, Islam Alexandrovich[1]; OLEJNIK, Andrej Vladimirovich[2*]

[1] IDTI RAS, Russia.

[2] MSUT “STANKIN”, Department of Management and Informatics in Technical Systems. Russia.

** Corresponding author*
e-mail: olejnikandrejv@yandex.ru

Received 06 August 2020; received in revised form 24 August 2020; accepted 04 September 2020

RESUMO

As peças tubulares com uma superfície externa com troca de calor aletada são geralmente produzidas pelo laborioso método de corte em tornos. Além disso, existe um método para a fabricação de aletas de alto desempenho por serrilhado a frio com serrilhados em anel o que, comparado com o corte, reduz a intensidade de trabalho de duas a seis vezes com um aumento significativo nas propriedades operacionais do produto. A desvantagem do método de serrilhado a frio com serrilhas de corte em anel pode ser defeitos de superfície indesejados e deformações de todo o produto. A obtenção de superfícies com alhetas em blanks de anel com alta qualidade superficial durante a serrilhagem requer um cálculo preciso da proporção de deformações longitudinais e transversais. Os fatores mais importantes que determinam a relação entre as deformações longitudinais e transversais (*rolling-out e rolling-off*) são o comprimento e a largura da superfície de contato. A necessidade de uma avaliação quantitativa dos parâmetros das deformações longitudinais e transversais determinou a finalidade deste manuscrito. O objetivo desse estudo foi desenvolver uma metodologia para calcular a superfície de contato de uma serrilha com um anel em branco (tubo) ao serrilhar com serrilhas de corte em anel. A metodologia proposta para calcular a superfície de contato da serra com um tubo ao serrilhar com serrilhas de corte em anel permite estimar a gama recomendada de tamanhos de tubos para serrilhar. Com base nas dependências mencionadas no manuscrito, os tamanhos-limite para tubos vazios foram calculados para garantir uma alheta de alta qualidade. Experimentos com o uso de aletas a frio em tubos com diferentes proporções de comprimento e diâmetro foram realizados, confirmando a possibilidade de utilizar a metodologia proposta para calcular a superfície de contato da serrilha com um tubo ao serrilhar aletas de troca de calor com serrilhas de corte em anel.

Palavras-chave: *alhetas externas, tubos vazios, zona de deformação.*

ABSTRACT

Tubular parts with an external finned heat-exchanging surface are usually produced by the laborious method of cutting on lathes. Besides, there is a method for the high-performance manufacturing of fins by cold knurling with ring-cut knurls, which, compared with cutting, reduces labor intensity by two to six times with a significant increase in the operational properties of the product. The disadvantage of the cold knurling method with ring-cut knurls can be unwanted surface defects and deformations of the entire product. Obtaining finned surfaces on ring blanks with high surface quality during knurling requires accurate calculation of the ratio of longitudinal and transverse strains. The most important factors determining the ratio of longitudinal and transverse strains (rolling-out and rolling-off) are the length and width of the contact surface. The need for a quantitative assessment of the parameters of longitudinal and transverse strains determined the purpose of this manuscript. This study aimed to develop a methodology for calculating the contact surface of a knurl with

DOI: 10.52571/PTQ.v17.n36.2020.387_Periodico36_pgs_372_389.pdf

a ring blank (pipe) when knurling with ring-cut knurls. The proposed method for calculating the knurl's contact surface with a tube when knurling with ring-cut knurls allows for estimating the recommended range of pipe sizes for knurling. Based on the dependencies mentioned in the manuscript, the limiting sizes for blank pipes were calculated to ensure high-quality finning. Experiments on cold rolling of ribbing on pipes with different lengths and diameter ratios were carried out, confirming the possibility of using the proposed methodology for calculating the knurl's contact surface with a pipe when knurling heat-exchanging finning with ring-cut knurls.

Keywords: *external finning, blank pipes, deformation zone.*

АННОТАЦИЯ

Трубчатые детали с наружной оребренной теплообменной поверхностью обычно изготавливают трудоёмким методом резания на токарных станках. Помимо этого, существует способ высокопроизводительного изготовления оребрения путем холодного накатывания роликами с кольцевой нарезкой, который по сравнению с резанием позволяет снизить трудоемкость в два-шесть раз при значительном повышении эксплуатационных свойств изделия. Недостатком метода холодного накатывания роликами с кольцевой нарезкой могут являться нежелательные дефекты поверхности и деформации всего изделия. Для получения на кольцевых заготовках оребрения с высоким качеством поверхности в процессе накатывания требуется точно рассчитывать соотношение продольной и поперечной деформаций. Важнейшими факторами, определяющими при этом соотношение продольной и поперечной деформаций (вытяжки и раскатки) являются длина и ширина контактной поверхности. Необходимость количественной оценки параметров продольной и поперечной деформаций определила цель настоящей работы. Целью данного исследования являлась разработка методики расчета параметров контактной поверхности ролика с кольцевой заготовкой (трубой) при накатывании оребрения роликами с кольцевой нарезкой. Предложенная в работе методика расчета контактной поверхности ролика с трубой при накатывании оребрения роликами с кольцевой нарезкой позволяет оценить рекомендуемый диапазон размеров трубы под накатывание оребрения. Используя полученные в работе зависимости выполнен расчет предельных размеров гладких труб, обеспечивающих качественное накатывание на них оребрения. Проведены эксперименты по холодной прокатке оребрения на трубах с различным соотношением длины и диаметра, подтверждающие возможность использования предложенной методики расчета контактной поверхности ролика с трубой при накатывании теплообменного оребрения роликами с кольцевой нарезкой.

Ключевые слова: *наружное оребрение, гладкие трубы, очаг деформации.*

1. INTRODUCTION:

Pipes with the external finned heat-exchanging surfaces (Figure 1) are used in many industries (Čarija *et al.*, 2014; Kuzma-Kichta *et al.*, 2007; Galushchak, 2017; Filippov, Cherepennikov and Leshchenko, 2010; Kim and Lee, 2013). The main areas of application for finned tubes are the machine-building industry uses them in refrigeration units, oil coolers, and compressors; chemical, oil refining, and petrochemical - in condensers, gas heaters and gas coolers; nuclear power - in gas coolers, intermediate refrigerators, steam air heaters, drying towers; in technology for air conditioning and in heat exchangers.

Finned tubes are monometallic or bimetallic structures consisting of two elements: an inner tube and outer ribs. The inner tube is a supporting element, through the inner cavity of which the working medium moves. It is made from metal, most often from steel. Cast iron and non-ferrous metals are used much less frequently. The material from which the inner part of the structure is made is resistant to temperature extremes and high pressure and has anti-corrosion properties (Sawicki and Dyja, 2010). The outer ribs can be made of steel, cast iron, and non-ferrous metals. The outer ribs efficiently transfer heat from the carrier.

To achieve the desired performance properties of the finned tube, appropriate materials are used. Ribbed tube heating elements are made of the following metals: cast iron (with magnesium and cerium); stainless steel, copper, brass, aluminum. In the manufacture of a bimetallic tube for heat exchangers, the layout of materials can be as follows (support tube + ribs): steel + aluminum; aluminum + aluminum; brass + aluminum (Wang *et al.,* 2013). The fins are often covered with a heat-resistant coating, which makes it possible to increase the heat transfer rate up to 55%. The previously degreased finned tube is coated with magnesium oxide, and subsequent annealing ensures heat resistance. Finned

bimetallic pipes are often coated with copper to prevent corrosion (Paquet, 1993).

There are several options for producing ribbed pipes (Kocurek and Adamiec, 2013). Depending on the method, the purpose of the products also differs. Ribbed tube heating elements are carried out in three main ways: rolling, winding, welding. Also, pipes with the external finned heat-exchanging surfaces are often obtained by cutting on screw-cutting machines and lathes. However, the complexity of finning, in this case, as a rule, is high.

Meanwhile, a known method of high-performance finning is cold knurling by ring-cut knurls. Compared with cutting, this method allows for reducing the complexity in two to six times with a significant increase in the operational properties of the product (Olejnik *et al.*, 2020). External finning of thin-walled products is usually done by ring-cut knurls. The process is based on the principle of self-tightening (screwing knurls into the turns). In this case, the billet or tool moves along with its axis at a constant distance between the axes of freely rotating knurls. The axes of the knurls are located at an angle corresponding to the elevation angle of the finning. Depending on the diameter of the billet, knurling can be done with a different number of knurls; their number increases with the increasing diameter of the billet. The first two to three turns of the knurling head are made with forced axial feed to ensure capturing the billet with -the knurls—further, billet self-tightens. Plastic deformation is done mainly by the tapered lead (conical) and partially calibrating (cylindrical) part of the knurl.

However, in the process of cold knurling, the finning itself can be deformed, its dimensions can change (Figure 2), as well as the diameter of the part's hole. This can be avoided by selecting the proper design of the hollow parts and using rigid mandrels inserted into the holes of the knurled part along with the sliding fit. Mandrels cause an increase in auxiliary time and often lead to their "being bit" during knurling. Also, difficulties often arise when removing mandrels.

Thin-walled hollow parts (pipes) can be finned by increasing the diameter of the billet, then the diameter of the billet is approximately taken equal to the average finning diameter. However, finning ring blanks with minimal ovality and high surface quality require accurate calculating the ratio of longitudinal and transverse strains at knurling. The most important factors determining the ratio of longitudinal and transverse strains (rolling-out and rolling-off) are the length and width of the contact surface. This problem has defined the purpose of this manuscript.

This study aimed to develop a methodology for calculating the contact surface of a knurl with a ring blank (pipe) when knurling with ring-cut knurls.

2. LITERATURE REVIEW:

An important mechanical engineering task is to reduce the amount of machining by cutting upon getting a billet approaching in shape and size to the finished product (Hakansson, 2015; Hitomi, 2017; Zheng, 2014; Semenov *et al.*, 2019b). As a result, there is the development of additive and hybrid shaping technologies, including pressure processing methods (Semenov *et al.*, 2019; Kopp, 1996; Kulikov *et al.*, 2016; Kulikov *et al.*, 2017). Simultaneously, engineers and technologists face tasks of increasing the efficiency of new technologies and reducing their implementation cost. The choice of a particular technology is determined by the design features of the manufactured product and economic feasibility and productivity (Alexandrov, Sheptunov, and Sannikov, 2019; Cherkashina, 2019).

Various technological methods can be used for external finning (Kulikov *et al.*, 2017). One of the external finning methods is the plastic deformation of metal in a hot or cold state (Sakai *et al.*, 2014). Using the plastic deformation method reduces processing waste, tool consumption, and labor costs. Thus, in most cases, the net cost of technological operations of external finning by cold knurling is much lower than cutting (Jiang, 2011). The reason for this is higher productivity of the method, a higher utilization rate of the processed material, lower costs for equipment depreciation, and replacement of the processing tool (Strycharska, 2019). If various defects often arise on the working surface during hot knurling as a result of heating and cooling the billet (scales, cracks, etc.), these defects are absent during cold knurling (Johnson, 2000; Liu, Tang, and Gu, 2014). Besides, cold plastic shaping has several significant technical advantages compared to cutting methods (Olejnik *et al.,* 2020).

Under pressure exceeding the stress value of the plastic flow of the processed material (Jiang, 2011), plastic deformation

(Johnson, 2000) occurs in it at room temperature, thus resulting in not only shaping but also a significant change in the material properties of the billet (McDowell and Moyar, 1991). A change in the properties of a deformed material is associated with changes in its structure that occur at various scale levels during the shaping of the final product (Kar'kina, Zubkova, and Yakovleva, 2013; Yakovleva, Kar'kina, and Zubkova, 2011; Qiao, Gao, and Starink, 2012). Peening at cold knurling helps in achieving an increase in the hardness and strength of the surface layer of the metal (Bower and Johnson, 1989; Yoshimi *et al.,* 2009). This greatly increases the wear resistance of the finning (Merkulov, 2008). The wear resistance of products obtained by plastic deformation is 30–40% higher than that obtained by cutting, and the strength characteristics are 10–20% higher (Song, Liu, and Tang, 2014). In addition to a significant change in the processed material properties under the influence of a smooth and practically non-deformable tool, the roughness of the processed surface decreases (Li, 2018).

External finning by cold knurling is not associated with heavy loads but is accompanied by a deformation of the metal. The maximum allowable deformation during cold knurling is determined by the plastic properties of the billet's material (Johnson, 2000). The metal extruded by the knurling tool flows upward. At the same time, as a result of feeding the knurls or the billet, the deformed metal flows axially in both directions, forming a wave in front of itself. Thus, manufacturing products with a finned heat-exchanging surface have the geometry of the knurled profile, which depends not only on the geometry of the knurling tool, but also on the laws of the metal flow process, which makes it necessary to analyze the processes occurring in the deformation zone during cold knurling (Salunke *et al.,* 2016).

3. MATERIALS AND METHODS:

This study seeks to solve the problem of determining the shape and area of the knurl's contact surface with a ring blank in the following formulation. The model approximation assumes that the elastic deformations of the tool and part are small. The knurl's contact surface with a ring blank is formed in the deformation zone from the cylindrical and conical parts of the tool. The generatrix of the contact surface of the ring blank and the knurl with ring turns is a broken line in longitudinal section a_1, a_2, a_3 … a_i (Figure 3).

The generatrix of the knurl's contact surface with the billet for its taper lead (conical) part is denoted by a straight line *AB*, located at an angle α to the billet's axis. The generatrix of the knurl's contact surface with the billet for its calibrating (cylindrical) part is denoted by a straight line *BC* parallel to the billet's axis.

The actual length of the contact surface along the finning surface exceeds the nominal length of the contact surface of the cylindrical and conical sections. To account for this difference, it is relevant to introduce two proportionality coefficients that separately consider the excess of the contact surface length for the conical η_{CON} and cylindrical η_{CYL} parts of the knurl, respectively. The length excess coefficient for the contact surface on the conical part of the knurl η_{CON} is defined by Eq. 1:

$$\eta_{CON} = L'_{1CON} / L_{1CON} \quad \text{(Eq. 1)}$$

where L'_{1CON} is the length of the actual contact finned surface along with the knurl's taper lead in the longitudinal section; L_{1CON} is the length of the straight conical section along with the apices of the forming tool in the longitudinal section.

The full application of the screw profile in the billet's metal is possible when its outer diameter is equal to or slightly less than the nominal diameter D_{CON1} of the conical part mouth of the tool along with the cutting dents. The actual length of the contact surface, in this case, is determined by Eq. 2:

$$L'_{1CON} = a_1 a_2 + n_{CON}\left(a_2 a_3 + a_3 a_4\right) \quad \text{(Eq. 2)}$$

where n_{CON} is the number of turns of the conical section; η_{CYL} coefficient considering the excess the contact length of the cylindrical section on the knurl's calibrating part is determined by Eq. 3:

$$\eta_{CYL} = L'_{CYL} / L_{CYL} \quad \text{(Eq. 3)}$$

where L'_{CYL} is the actual length of the contact finned surface along with the cylindrical part of the knurl; L_{CYL} is the length of the cylindrical part of the knurl and the finning apices of the tool.

Provided that the screw profile of the tool is completely filled with the billet's metal, the length of the actual contact surface in the longitudinal section L'_{CYL} is determined by Eq. 4:

$$L'_{CYL} = n_{CYL}\left(Bb_1 + b_1b_2\right) \quad \text{(Eq. 4)}$$

where n_{CYL} is the number of turns at the cylindrical (calibrating) part of the tool.

Next, it is relevant to determine the contact surface of the billet with a smooth roller (i.e., to a first approximation, without ring cutting). In the process of continuous longitudinal movement of the billet, the generatrix of the contacting conical section *AB* (Figure 4), before meeting the next knurl, will take the position *A′B′*. With a sufficient degree of accuracy, then it can be assumed that the generatrix of the billet's conical section, *A′B′*, is a straight line. Accordingly, *AA′* is the axial feed of the billet S_Z to one knurl, and *BB′* is the total linear displacement of the metal equal to the product of $S_Z \cdot \mu_\Sigma$, where μ_Σ is the total rolling-out of the tubular billet in the longitudinal section, determined by Eq. 5:

$$\mu_\Sigma = D_{BM}\, t_P / D_{PM}\, t_P \quad \text{(Eq. 5)}$$

where D_{BM} is the mean diameter of a billet to be knurled; D_{PM} is the mean diameter of a knurled part t_B is the wall thickness of the billet; t_P is the wall thickness of the processed part.

The contact surface of the smooth roller and the ring blank is formed by the intersection of the following surfaces: billet's cylinder/cone of the smooth roller; ring blank cone/knurl cone; ring blank cone/knurl cylinder. Accordingly, the contact surface is divided into sections L_1, L_2 and L_3, each of which is determined according to Eqs. 6a-c:

$$L_1 = S_Z \quad \text{(Eq. 6a)}$$

$$L_2 = \frac{D_B - D_O - D_P}{2\mathrm{tg}\,\alpha} - S_Z = \frac{t_B - t_P + \Delta}{\mathrm{tg}\,\alpha} - S_Z \quad \text{(Eq. 6b)}$$

$$L_3 = S_Z\,\mu_\Sigma \quad \text{(Eq. 6c)}$$

where L_1 is the length of the smooth knurl's contact with the ring blank at the *AA′* section; L_2 is the length of the smooth knurl's contact with the ring blank at the *A′B* section; L_3 is the length of the smooth knurl's contact with the ring blank at the *BB′* section.

The total length of the contact surface *L* is obtained by summing L_1, L_2 and L_3:

$$L = \frac{\left(D_o - D_T\right)\left(t_B - t_p + 1\right)}{2\mathrm{tg}\,\alpha} + S_Z\mu_\Sigma = \frac{\Delta\left(t_\Sigma + 1\right)}{\mathrm{tg}\,\alpha} + S_Z\mu_\Sigma \quad \text{(Eq. 7)}$$

where $\Delta t_\Sigma = t_B - t_P$; $\Delta = (D_0 - D_P)/2$.

The expression of the total length of the contact surface is valid for the case when the generatrix of the conical and cylindrical sections of the contact surface in a longitudinal section are straight lines. In this case, the generators of the conical and cylindrical sections have the form of broken lines corresponding to the cross-section of the profile of the turns of the knurls. In particular, the profile of the knurl (Figure 3) can serve for finning in the form of an isosceles triangle with an angle between the sides of 55° and with rounded peaks of radius *r* and spacing *S*.

To determine the contact surface of the ring blank with a ring cut knurl, it turns to Figure 4, which shows a longitudinal section of the deformation zone and a vertical projection of the longitudinal section of the contacting sections. In the process of continuous longitudinal movement of the billet, the generatrix of the contacting conical part of the knurl, before meeting the next knurl, will assume a position similar to processing with a smooth roller. The only difference is that the generatrix of the conical and cylindrical sections of the knurl is a broken line.

Thus, the total rolling-out of the tubular billet in the longitudinal direction can be determined by Eq. 8, which is similar to Eq. 1, but has different values of some parameters included in it:

$$\mu'_\Sigma = \frac{D'_{BM}\, t_B}{D'_{PM}\, t'_P} \quad \text{(Eq. 8)}$$

where μ'_Σ is total rolling-out of ring blank in the longitudinal direction at knurling finning by the ring-cut knurls; D'_{BM} is the mean diameter of a ring blank; D'_{PM} is the mean diameter of a knurled heat-exchanging part, determined by Eq. 9:

$$D'_{PM} = D_{PM} + t_2 / 4 \quad \text{(Eq. 9)}$$

where D_{PM} is the mean radius of the pipe without threading; t_2 is the finning height.

Since the midline of the profile is approximately symmetrical to its height, the value of t'_P is determined by Eq. 10, where t_P

denotes the minimum wall thickness of the ring blank at the finning:

$$t'_{\text{P}} = t_{\text{P}} + t_2 / 4 \qquad \text{(Eq. 10)}$$

Using the above formulas, the final dependence for determining the total rolling-out of the rolling-out in the process of finning on it is obtained (Eq. 11):

$$\mu'_{\Sigma} = \frac{D'_{\text{BM}}\, t_{\text{B}}}{\left(D_{\text{PM}} + \frac{t_2}{2}\right)\left(t_{\text{P}} + \frac{t_2}{2}\right)} \qquad \text{(Eq. 11)}$$

The contact surface of a roller having an annular cut with a tubular billet is formed by the intersection of the surfaces of the cylindrical part of the billet and the conical part of the knurl; the conical part of the ring blank and the conical part of the knurl; the conical part of the ring blank and the cylindrical part of the knurl. Therefore, by analogy with (6), the contact surface can be conditionally divided into sections L'_1, L'_2 and L'_3, the length of each of which is determined in accordance with Eqs. 12a-c:

$$L'_1 = S / z \qquad \text{(Eq. 12a)}$$

$$L'_2 = \frac{D_{\text{B}} - D_{\text{O}} - D_{\text{M}}}{2\text{tg}\,\alpha} - \frac{S}{z} = \frac{t_{\text{B}} - t_{\text{M}} + \Delta}{\text{tg}\,\alpha} = \frac{\Delta t_{\Sigma} + \Delta}{\text{tg}\,\alpha} - \frac{S}{z} \qquad \text{(Eq. 12b)}$$

$$L'_3 = S\mu_{\Sigma} / z \qquad \text{(Eq. 12c)}$$

where S is the finning spacing; z is the number of knurls in the knurling head.

After adding the lengths of the sections L'_1, L'_2 and L'_3, it is obtained the total length of the contact surface (Eq. 13):

$$L' = \frac{\Delta t_{\Sigma} + \Delta}{\text{tg}\,\alpha} + \frac{S}{z}\mu_{\Sigma} \qquad \text{(Eq. 13)}$$

Considering the coefficients of exceeding the lengths of the contact surface, Eqs. 12a-c can be rewritten in the following form (Eqs. 14a-c):

$$L'_1 = S\eta_{\text{CON}} / z \qquad \text{(Eq. 14a)}$$

$$L'_2 = \eta_{\text{CON}}\left(\frac{\Delta t_{\Sigma} + \Delta}{\text{tg}\,\alpha} - \frac{S}{z}\right) \qquad \text{(Eq. 14b)}$$

$$L'_3 = \mu_{\Sigma}\,\eta_{\text{CYL}} S / z \qquad \text{(Eq. 14c)}$$

After substitution and transformations, Eq. 13 for determining the total length L' takes the form of Eq. 15:

$$L = \eta_{\text{CON}}\frac{\Delta t_{\Sigma} + \Delta}{\text{tg}\,\alpha} + \frac{S\mu_{\Sigma}\,\eta_{\text{CYL}}}{z} \qquad \text{(Eq. 15)}$$

Final determination of the contact surface length of the knurl with a thin-walled ring blank requires expressing the unknown coefficients η_{CON} and η_{CYL} in terms of the known parameters of the knurl, i.e. through r, ε, H, S (Figure 5).

Determining the contact length of the cylindrical section in the longitudinal section does not present significant difficulties if one singles out the profile of one turn, designating its elements in the most general form (Figure 5a). This requires determining archs $\smile BM$, $\smile EB_1F$ and $\smile NB_2$, and segments ME and FN. Following Figure 5, one can write the geometric dependences (Eqs. 16a-c), which ultimately allow for obtaining the dependence (Eq. 16d):

$$OG = EG\sin\varepsilon/2 = r\sin\varepsilon/2 \qquad \text{(Eq. 16a)}$$

$$GG = \frac{H}{n} + r \qquad \text{(Eq. 16b)}$$

$$CO = GG - OG \qquad \text{(Eq. 16c)}$$

$$CO = H / n + r\left(1 - \sin\varepsilon/2\right) \qquad \text{(Eq. 16d)}$$

where n defines CB_1 distance.

Knowing CO, it is easy to find that $EC = AM = ND$ can be expressed by Eq. 17:

$$EC = \frac{CO}{\cos\left(\varepsilon/2\right)} = \frac{\left(H / n\right) + r\left[1 - \sin\left(\varepsilon/2\right)\right]}{\cos\left(\varepsilon/2\right)} \qquad \text{(Eq. 17)}$$

Since the segment $ME = AC - 2EC$, then EM is expressed by Eq. 18:

$$EM = \frac{S}{2\sin\left(\varepsilon/2\right)} - 2\frac{\left(H / n\right) + r\left[1 - \sin\left(\varepsilon/2\right)\right]}{\cos\left(\varepsilon/2\right)} \qquad \text{(Eq. 18)}$$

Figure 5a shows that $\smile BN = \smile EB_1F / 2 = \smile NB_2$, i.e. it is sufficient to determine only one of these values (Eq. 19):

$$LEGF = 2\left(90° - \varepsilon/2\right) = 180° - \varepsilon \quad \text{(Eq. 19)}$$

Thus, Eq. 20 is obtained, and the contact length of one turn in the cylindrical section, respectively, is expressed by Eq. 21:

$$\smile EB_1F = \frac{2\pi r\left(180° - \varepsilon\right)}{360°} = \frac{\pi r\left(180° - \varepsilon\right)}{180°} \quad \text{(Eq. 20)}$$

$$L'_{\text{CYL}} = 2\left(ME + EB_1F\right) \quad \text{(Eq. 21)}$$

Substituting the previously found values (Eq. 18) and (Eq. 20) into Eq. 21, it is obtained the dependence (Eq. 22):

$$L'_{\text{CYL}} = \frac{S}{\sin\left(\varepsilon/2\right)} + \frac{\left(2H/n\right) + 2r\left[1 - \sin\left(\varepsilon/2\right)\right]}{\cos\left(\varepsilon/2\right)} + \frac{\pi r\left(180° - \varepsilon\right)}{90°} \quad \text{(Eq. 22)}$$

After substituting the L'_{CYL} value in Eq. 3, taking into account the number of turns of the profile on the cylindrical part, it is found the excess coefficient of the contact length of the cylindrical section in the deformation zone (Eq. 23):

$$\eta_{\text{CYL}} = \frac{L'_{\text{CYL}}}{L_{\text{CYL}}} n_{\text{CYL}} \quad \text{(Eq. 23)}$$

where n_{CYL} is the number of turns at the cylindrical section of the knurl.

$$L'_{\text{CYL}} = Sn_{\text{CYL}} \quad \text{(Eq. 24)}$$

By substituting the found values into Eq. 23, and the following is obtained (Eq. 25) after the transformations:

$$\eta_{\text{CYL}} = \frac{1}{\sin\left(\varepsilon/2\right)} - \frac{2H + 2rh\left[1 - \sin\left(\varepsilon/2\right)\right]}{Sh\cos\left(\varepsilon/2\right)} + \frac{\pi r}{90}\left(180° - \varepsilon\right) \quad \text{(Eq. 25)}$$

It is often more convenient, without setting the parameters *r* and *H*, to find the η_{CYL} value through the parameters *S* and ε. In this case, Eq. 25 will take the following form (Eq. 26):

$$\eta_{\text{CYL}} = \frac{1}{\sin\left(\varepsilon/2\right)} - \frac{2\left[S - \cos\left(\varepsilon/2\right)\right]}{n\cos\left(\varepsilon/2\right)\text{ctg}\left(\varepsilon/2\right)} + \frac{\pi\left(180° - \varepsilon\right)}{90°}\frac{S - 2\cos\left(\varepsilon/2\right)}{2Sn\left[\text{ctg}\left(\varepsilon/2\right) - \cos\left(\varepsilon/2\right)\right]} \quad \text{(Eq. 26)}$$

The final values of the parameters *H* and *r* are determined in *S* and ***ε***, since the transformations are simple and cumbersome, the intermediate derivation of Eqs. 27a and 27b is not presented:

$$H = S/2\text{ctg}\left(\varepsilon/2\right) \quad \text{(Eq. 27a)}$$

$$r = \frac{S - 2\cos\left(\varepsilon/2\right)}{2n\,\text{ctg}\left(\varepsilon/2\right)\left[1 - \sin\left(\varepsilon/2\right)\right]} \quad \text{(Eq. 27b)}$$

When determining the contact length of one turn of the profile on the conical section of the contact surface in the deformation zone, it should be remembered that the generatrix of the conical section, having an angle α with the knurl's axis, somewhat distorts the profile of the turn. It has to be determined the maximum value of the contact length of one turn of finning, taking into account the distortion of the latter in the conical section. Consider the profile of a single turn (Figure 5b-c) for this. Since the turns profile on the knurl's conical part is inclined relative to the profile of the turn of the cylindrical part, provided that the finning spacing *S* and the rounding radius of the vertices *r* and dents on both parts of the knurl are maintained, the sides of the profile of the turn at the finned heat transfer strand will have different tilt angles relative to the centerline *CC'*: $\varepsilon_{1/2}$ and $\varepsilon_{2/2}$. It is known that the angle between the tangent and the chord is measured by half of the arc enclosed inside the central angle. Therefore, the straight line E_1F_1, resting at the tangency points on two chords located symmetrically to the chord *EF* intersects each chord at the point of tangency at an angle of $\alpha/2$. If one assumes that $E_1\sigma_2 \approx EO$ and considering that the intersection angle equals to $\alpha/2$, then the equation $\sigma_2 O \approx EO \cdot \text{tg}(\alpha/2)$ can be written like that, but since $EO \approx r \cdot \text{tg}(\alpha/2)$, then $\sigma_2 O \approx r \cdot \cos(\varepsilon/2) \cdot \text{tg}(\alpha/2)$. The value $E_1\sigma_2$ can be specified in the following way: $E_1\sigma_2 \approx EO - EE'' = r(\cos(\varepsilon/2) - \sin(\varepsilon/2) \cdot \text{tg}(\alpha/2))$. At that, $EE'' \approx \sigma_2 O \cdot \text{tg}(\varepsilon/2)$. Accordingly, the unknown angle $\angle\sigma_2 E_1 i_2$ (Figure 5c) one defines by equality (Eq. 28a), and the analytical value of the angle is expressed through the inverse trigonometric function (Eq. 28b):

$$\cos(\varepsilon_1/2) \equiv \sigma_2\varepsilon/2 = \cos(\varepsilon/2) - \sin(\varepsilon/2)\,\mathrm{tg}(\alpha/2)$$ (Eq. 28a)

$$\varepsilon_1 = 2\arccos\left[\cos(\varepsilon/2) - \sin(\varepsilon/2)\,\mathrm{tg}(\alpha/2)\right]$$ (Eq. 28b)

The unknown angle $\angle\sigma_2E_1i_2$ will be defined in the same way, with the purpose of what one preliminary defines K_2F_1:

$$K_2F_1 \equiv FO + F''F_1 = r\left[\cos(\varepsilon/2) + \sin(\varepsilon/2)\,\mathrm{tg}(\alpha/2)\right]$$ (Eq. 29)

Since $FO = r\cdot\cos(\varepsilon/2)$, a $F''F_1 = E''E_1 = r\cdot\cos(\varepsilon/2)\cdot\mathrm{tg}(\alpha/2)$, then the analytical value of the ε_2 angle will be expressed as the inversed trigonometric function (Eq. 30):

$$\varepsilon_2 = 2\arccos\left[\cos(\varepsilon/2) - \sin(\varepsilon/2)\,\mathrm{tg}(\alpha/2)\right]$$ (Eq. 30)

The obtained expressions (Eq. 28b) and (Eq. 30) allow for determining the length of the contact arcs of the profile turn on the conical part of the knurl (Eq. 31a) and (Eq. 31b):

$$\cup E_1a_3 \equiv \cup N_1a_4 = \frac{\pi r\varepsilon_1}{360°}$$ (Eq. 31a)

$$\cup F_1a_3 \equiv \cup N_1a_4 = \frac{\pi r\varepsilon_2}{360°}$$ (Eq. 31b)

The lengths of the contact lengths are expressed in terms of known values by Eqs. 32a and 32b:

$$M_1E_1 = \frac{S\mathrm{tg}\alpha + 2H(1-2/n) - 4r\left[1-\sin(\varepsilon_1/2)\right]}{2\cos(\varepsilon_1/2)}$$ (Eq. 32a)

$$F_1N_1 = \frac{S\mathrm{tg}\alpha + 2H(1-2/n) - 4r\left[1-\sin(\varepsilon_2/2)\right]}{2\cos(\varepsilon_2/2)}$$ (Eq. 32b)

The maximum contact length of one turn of the profile on the conical section L'_{CON1} can be determined by Eq. 33a. After substitution in Eq. 33a of values M_1E_1 и F_1N_1, Eq. 33b is obtained:

$$L'_{CON1} = 2\cup E_1a_3 + 2\cup F_1a_3 + F_1N_1 + E_1M_1$$ (Eq. 33a)

After that, taking into account the number of turns on the conical part of the knurl, one finds the value of the coefficient of the contact length excess of the conical section in the deformation zone (Eq. 34):

$$\eta_{CON} = \frac{L'_{1CON}n_{CON}}{L_{1CON}} = \frac{L'_{1CON}n_{CON}\cos\alpha}{S\,n_{CON}}$$ (Eq. 34)

where n_{CON} is the number of turns at the conical section of $L_{CON} = S\cdot n_{CON}$. In the end, Eq. 34 will take the form shown in the appendix (Eq. 35).

The width of the contact surface b_X can be determined using the following formula (Eq. 36):

$$b_X = \sqrt{\delta t_X \frac{Dd}{D+d}}$$ (Eq. 36)

where D is the knurl's engagement diameter, calculated according to the formula $D = D_1 - \xi(D_H - d_1)$; d is the engagement diameter of the finning, which is equal to $d = d_1 - \xi(D_H - d_1)$; δt_X is the reduction in the section; ξ is the engagement coefficient depending on the profile; D_H is outer diameter along with the vertices; D_1 is the knurl's outer diameter; d_1 is the inner diameter along with the dents.

It is known that the rotation from the knurks to the deformable part during the knurling is transmitted without slipping only in section along the height of the profile. The diameters of the knurls and parts corresponding to this section are the engagement radii. Suppose one assumes that the specific forces during plastic deformation on the contact surfaces are equal along the entire profile. In that case, the magnitude of the engagement diameter is determined from the condition of equality of sliding friction over sections of the profile that lie above and below the engagement radius. Therefore, calculation of the width of the contact surface uses the engagement diameters presented in the formula D и d.

Reduction size at the borders of the sections L_1 and L_2 (Figure 4), respectively, will be determined by Eq. 37a, and at the borders of the sections L_2 and L_3 – by Eq. 37b.

$$\delta t_1 = m\eta_{CON}\,\mathrm{tg}\alpha$$ (Eq. 37a)

$$\delta t_2 = \frac{m\mu_\Sigma\eta_{CON}\eta_{CYL}(\Delta t_\Sigma + \Delta)\mathrm{tg}\alpha}{\eta_{CON}(\Delta t_\Sigma + \Delta) + m(\mu_\Sigma\eta_{CYL} - \eta_{CON})\mathrm{tg}\alpha}$$ (Eq. 37b)

Further, analyzing the ratio (Eq. 38)

$$\frac{\delta t_2}{\delta t_1} = \frac{\mu_\Sigma \left(\Delta t_\Sigma + \Delta\right)}{\left(\Delta t_\Sigma + \Delta\right) + m\left(\mu_\Sigma - 1\right)\mathrm{tg}\alpha} \quad \text{(Eq. 38)}$$

At $\Delta = 0$ and $D_B = D_P$, $\mu_\Sigma = t_B/t_P$. Then $\delta t_2/\delta t_1 = t_B / (t_P + m \cdot \mathrm{tg}\alpha)$.

At $(m \cdot \mathrm{tg}\alpha) < \Delta t_\Sigma$ the ratio is $(\delta t_2 / \delta t_2) > 1$, i.e. the minimum reduction corresponds to the section limits L_2 and L_1. The width of the deformation zone at the border of each section (Eq. 39a) and (Eq. 39b):

$$b_1 = \sqrt{\frac{m\eta_{CON} D_{LIM}\,\mathrm{tg}\alpha}{2}} \quad \text{(Eq. 39a)}$$

$$b_2 = \frac{mD_{LIM}\mu_\Sigma \eta_{CON}\eta_{CYL}\left(\Delta t_\Sigma + \Delta\right)\mathrm{tg}\alpha}{2\eta_{CON}\left(\Delta t_\Sigma + \Delta\right) + m\left(\mu_\Sigma \eta_{CYL} - \eta_{CON}\right)\mathrm{tg}\alpha} \quad \text{(Eq. 39b)}$$

Thus, Eqs. 1-39 determine all the characteristic dimensions of the metal contact surface of ring blank with knurls, the horizontal projection of which resembles a curved trapezoid in shape.

4. RESULTS AND DISCUSSION:

The main task when introducing the process of rolling ribs is to achieve the required accuracy of the workpiece. The main reason for the formation of defects during the technological process of rolling is associated with the conditions for forming rib profiles. Extrusion of the profile is carried out due to the redistribution of elementary volumes of metal, displaced by the working turns of the forming tool. In the process of extrusion of the profile, both symmetric and asymmetric deformation may occur. The nature of the deformation depends on the path of the working turns of the rolling tool along the surface of the formed rib. The formation of defects at the top of the rib profile is possible due to symmetric deformation. However, defects on the rib profile can have a different location, depending on the amount of displacement of the tool profile in the deformation cycle. Controlling deformed metal flow is an important condition for the rolling process (Jiang *et al.*, 2010; Feng and Wang, 2004; Zhang *et al.*, 2014; Aljabri, Jiang and Wei, 2014).

The experimental studies of the imprints of the contact surface of the knurled billet confirmed the correctness of the proposed methodology and formulas for calculating the contact surface of metal with the knurl. Since in oractice $m\eta_{CON} << \eta_{CON}(\Delta t_\Sigma + \Delta)/\mathrm{tg}\alpha$, i.e. $L_1 << L_2 + L_1$, then, without a large error, the sides of the trapezoid can be straightened, and then the vertical and horizontal projections of the contact surface of the billet's metal with the knurl are determined by Eqs. 40a and 40b:

$$F_{VERT} = \frac{\delta t_1 b_1 + b_2 \delta t_2 + \left(b_1 + b_2\right)\left(\Delta t_\Sigma + \Delta\delta t_2 - \delta t_2\right)}{2} \text{(Eq. 40a)}$$

$$F_{HOR} = \frac{\left(L_1 b_1 + L_3 b_2\right) + L_2\left(b_1 + b_2\right)/2}{2} \quad \text{(Eq. 40b)}$$

As it can be seen from Figure 5, filling strands in the deformation zone depends on the billet's diameter: the larger its diameter, the larger the filling strands is, and the more contact has the billet with the knurl, and the larger the billet coverage perimeter of the knurl is. and the higher the η_{CON} and η_{CYL} coefficients are. Accordingly, for certain ratios of diameter to wall thickness, the diameter of a thin-walled pipe should vary from D'_{BMIN} to D'_{BMAX} (Figure 6), where D'_{BMIN} is the minimum outer diameter of the blank pipe to be knurled; D'_{BMAX} is the maximum outer diameter of the blank pipe to be knurled. In this case, the minimum diameter of the pipe D'_{BMIN} should, accordingly, be in the range from the minimum outer finning diameter d'_{0MIN} to the maximum finning diameter d'_{0MAX}. If the minimum outer diameter of the pipe is determined by the outer largest mouth diameter of the working solution D_{CON1} of the knurl's conical part during their installation (Figure 6), then $D_{BMAX} \le D_{CON1}$. Thus, the larger the billet's diameter, the greater the η_{CON} and η_{CYL} values in Eqs. 12a-c, and since $\eta_{CON} > 1$ and $\eta_{CYL} > 1$, the contact surface length L increases with increasing billet's diameter.

Analysis of Eqs. 37a, b allows for stating that with an increase in the billet's diameter, the amount of compression at the boundary of the sections L_1 and L_2, as well as L_2 and L_3 also increases. Thus, the length of the contact surface with a certain ratio of diameter to wall thickness increases with increasing billet's diameter from minimum to maximum. Similarly, with an increase in the length of the contact surface, the number of compression increases. The reduction, according to Eqs. 37a, b increases with increasing billet's diameter from minimum to maximum. It is known that the knurling force P_{ROL} directly depends on the width

and length of the contact surface, i.e. $P_{ROL} = \rho F_C$, where ρ are specific pressing forces at knurling; F_C is the contact area. Respectively, at ρ = const there are the following ratios of the forces: $P_{ROL} > P_{ROL}$ at $F > F_C$; $P_{ROL} < P_{ROL}$ at $F < F_C$. Thus, the knurling force will increase with increasing length of the contact surface, which is ultimately proportional to the billet's diameter (in a wide range of diameter to wall thickness ratios).

Cold plastic deformation has a significant effect on the physical and mechanical properties, macro- and microstructure of the processed metal. As a result of cold deformation, the initial metal, which had properties approximately the same in different directions and a chaotically oriented structure, receives a directionally oriented fibrous structure and increased anisotropic mechanical characteristics. The change in metal properties depends on the degree of plastic deformation, with an increase in which all characteristics of the metal's resistance to deformation increase, namely, the strength of the metal increases, and the hardness and fluidity increase. At the same time, the values of plasticity decrease: the relative elongation and impact strength decrease. The effect of cold plastic deformation on the surface quality of parts is especially significant.

5. CONCLUSIONS:

Method for the high-performance manufacturing of fins by cold knurling, compared with cutting, reduces labor intensity by two to six times with a significant increase in the operational properties of the product. The disadvantage of the cold knurling method with ring-cut knurls can be unwanted surface defects and deformations of the entire product. Obtaining finned surfaces on ring blanks with high surface quality during knurling requires for accurate calculation of the ratio of longitudinal and transverse strains.

The manuscript proposed a method for calculating the knurl's contact surface with a pipe when knurling with ring-cut knurls, which allows for estimating the recommended range of pipe sizes for knurling. Based on the above-listed dependencies, the limiting sizes for blank pipes were calculated to ensure high-quality finning. The authors experimented with cold finning on pipes with different length and diameter ratios, confirming the possibility of using the proposed methodology for calculating the knurl's contact surface with a pipe when finning with ring-cut knurls. The main reason for the formation of defects during the technological process of rolling is associated with the conditions for the formation of rib profiles. Extrusion of the profile is carried out due to the redistribution of elementary volumes of metal, displaced by the working turns of the forming tool. It should be noted that the most important factors determining the ratio of longitudinal and transverse strains (rolling-out and rolling-off) are the length and width of the contact surface. No defects are observed at the ribs under the recommended rolling conditions.

6. ACKNOWLEDGEMENTS:

Some results of this manuscript were obtained as part of the work under the Agreement on the provision of subsidies under date of 13 December 2019 No. 075-15-2019-1941 (the agreement internal number 05.607.21.0321) on the topic: “Development of design and technological solutions for modular prefabricated transmission line towers with integrated systems for continuous digital monitoring of the condition and thermal stabilization of the soil to meet the needs of the Arctic regions and the Far North” with the Ministry of Science and Higher Education of the Russian Federation. The unique identifier of the applied research (project) is RFMEFI60719X0321.

7. REFERENCES:

1. Alexandrov, I.A., Sheptunov, S.A. and Sannikov, A.S. (2019, 23-27 September). *Some approaches to the formalization principles of achieving the target properties of products in the automation of technological processes in mechanical engineering*. Paper presented at the International Conference “Quality Management, Transport and Information Security, Information Technologies”. doi:10.1109/itqmis.2019.8928338
2. Aljabri, A., Jiang, Z.Y., and Wei, D.B. (2014). Analysis of Thin Strip Profile during Asymmetrical Cold Rolling with Roll Crossing and Shifting Mill. *Advanced Materials Research*, 894, 212–216. doi: 10.4028/www.scientific.net/amr.894.212
3. Bower, A.F. and Johnson, K.L. (1989). The influence of strain hardening on

cumulative plastic deformation in rolling and sliding line contact. *Journal of the Mechanics and Physics of Solids, 37*(4), 471-493. doi:10.1016/0022-5096(89)90025-2

4. Čarija Z., Franković B., Perčić M., and Čavrak M. (2014). Heat transfer analysis of fin-and-tube heat exchangers with flat and louvered fin geometries. *International Journal of Refrigeration*, 45, 160–167. doi:10.1016/j.ijrefrig.2014.05.026
5. Cherkashina, O. (2019). Management of quality of technological processes in mechanical engineering using three-parameter modeling. *Engineering*, 23, 159–165. doi:10.32820/2079-1747-2019-23-159-165
6. Feng, C.-X.J., and Wang X.-F. (2004). *Data mining techniques applied to predictive modeling of the knurling process*. IIE Transactions, 36(3), 253–263. doi: 10.1080/07408170490274214
7. Filippov, E.B., Cherepennikov, G.B., and Leshchenko, T.G. (2010). A numerical study of the thermal efficiency of a tubular heating surface with split spiral-tape finning. *Thermal Engineering*, 57(7), 598–602. doi:10.1134/s0040601510070116
8. Galushchak, I. (2017). Experimental investigation of heat transfer in interfin channels of punched spiral tube finning. *Technology Transfer: Fundamental Principles and Innovative Technical Solutions*, 12–14. doi:10.21303/2585-6847.2017.00473
9. Hakansson, H. (2015). *Industrial technological development (Routledge revivals): A network approach.* London, United Kingdom: Routledge. doi:10.4324/9781315724935
10. Hitomi, K. (2017). *Manufacturing systems engineering.* London, United Kingdom: Routledge. doi:10.1201/9780203748145
11. Jiang, Z.Y. (2011). Mechanics of cold rolling of thin strip. In J. Awrejcewicz (Ed.). *Numerical analysis: Theory and application.* IntechOpen. doi:10.5772/23344
12. Jiang, Z.Y., Du, X.Z., Du, Y.B., Wei, D.B., and Hay, M. (2010). Strip Shape Analysis of Asymmetrical Cold Rolling of Thin Strip. *Advanced Materials Research*, 97-101, 81–84. doi:10.4028/www.scientific.net/amr.97-101.81
13. Johnson, K.L. (2000). Plastic deformation in rolling contact. In B. Jacobson and J.J. Kalker (Eds.), *Rolling contact phenomena* (Vol. 411, pp. 163-201). Vienna, Austria: Springer. doi:10.1007/978-3-7091-2782-7_3
14. Kar'kina, L.E., Zubkova, T.A. and Yakovleva, I.L. (2013). Dislocation structure of cementite in granular pearlite after cold plastic deformation. *The Physics of Metals and Metallography, 114*(3), 234-241. doi:10.1134/s0031918x13030095
15. Kim, K., and Lee, K.-S. (2013). Frosting and defrosting characteristics of surface-treated louvered-fin heat exchangers: Effects of fin pitch and experimental conditions. *International Journal of Heat and Mass Transfer*, 60, 505–511. doi:10.1016/j.ijheatmasstransfer.2013.01.036
16. Kocurek, R., and Adamiec, J. (2013). Manufacturing Technologies of Finned Tubes. *Advances in Materials Sciences*, 13(3). doi:10.2478/adms-2013-0009
17. Kopp, R. (1996). Some current development trends in metal-forming technology. *Journal of Materials Processing Technology, 60*(1-4), 1-9. doi:10.1016/0924-0136(96)02301-1
18. Kulikov, M.Y., Larionov, M.A., Sheptunov, S.A. and Gusev, D.V. (2016, 4-11 October). *The influence of pre-settings of the automated system rapid prototyping on the qualitative characteristics of formation.* Paper presented at the IEEE Conference on Quality Management, Transport and Information Security, Information Technologies. doi:10.1109/itmqis.2016.7751916
19. Kulikov, M.Y., Sheptunov, S.A., Larionov, M.A. and Gusev, D.V. (2017, 24-30 September). *Manufacturing of highquality products to the method of DLP RP — Technology.* Paper presented at the International Conference "Quality

Management, Transport and Information Security, Information Technologies". doi:10.1109/itmqis.2017.8085932

20. Kulikov, M.Y., Yagodkin, M.V., Larionov, M.A. and Sheptunov, S.A. (2017, 24-30 September). *The anodic mechanical machining application for thread cutting of small diameters.* Paper presented at the International Conference "Quality Management, Transport and Information Security, Information Technologies". doi:10.1109/itmqis.2017.8085931
21. Kuzma-Kichta, Y.A., Savel'ev, P.A., Koryakin, S.A., and Dobrovol'skii, A.K. (2007). Studying of heat-transfer enhancement in tubes with screw knurling. *Thermal Engineering*, 54(5), 407–409. doi:10.1134/s0040601507050138
22. Li, Z. (2018). Elastic deformation of surface topography under line contact and sliding-rolling conditions. *Journal of Mechanical Engineering, 54*(5), 142-148. doi:10.3901/jme.2018.05.142
23. Liu, B., Tang, C.L. and Gu, T.Q. (2014). A method to avoid strip breakage for thin strip steel in cold rolling. *Advanced Materials Research, 1004-1005*, 1211-1215. doi:10.4028/www.scientific.net/amr.1004-1005.1211
24. McDowell, D.L. and Moyar, G.J. (1991). Effects of non-linear kinematic hardening on plastic deformation and residual stresses in rolling line contact. *Wear, 144*, 19-37. doi:10.1016/b978-0-444-88774-0.50006-7
25. Merkulov, D.V. (2008). Pipe rolling in helical-rolling mills without a guide system. *Steel in Translation*, 38(7), 580–584. doi:10.3103/s096709120807022x
26. Olejnik, A.V., Kapitanov, A.V., Alexandrov, I.A. and Tatarkanov, A.A. (2020a). Calculation methodology for geometrical characteristics of the forming tool for rib cold rolling. *Journal of Applied Engineering Science, 18*(2), 292-300. doi:10.5937/jaes18-25211
27. Qiao, X.G., Gao, N. and Starink, M.J. (2012). A model of grain refinement and strengthening of Al alloys due to cold severe plastic deformation. *Philosophical Magazine, 92*(4), 446-470. doi:10.1080/14786435.2011.616865
28. Paquet, A. (1993). Comparison of Brazing Processes for Aluminum Heat Exchanger Manufacturing. *SAE Technical Paper Series*. doi:10.4271/931093
29. Sakai, T., Belyakov, A., Kaibyshev, R. and Miura, H. (2014). Dynamic and post-dynamic recrystallization under hot, cold and severe plastic deformation conditions. *Progress in Materials Science, 60*, 130-207. doi:10.1016/j.pmatsci.2013.09.002
30. Salunke, K.A., Lambhate, V., Jadhav, U., and Kumbhar, S. (2016). Optimization of Pipe Finning Process with Engineering Principles. *International Journal of Science and Research (IJSR)*, 5(3), 270–272. doi:10.21275/v5i3.nov161849
31. Sawicki, S., and Dyja, H. (2010). Theoretical and Experimental Analysis of the Bimetallic Ribbed Bars Steel - Steel Resistant to Corrosion Rolling Process. *Archives of Metallurgy and Materials*, 57(1). doi:10.2478/v10172-011-0153-2
32. Song, M., Liu, X.H., and Tang, D.L. (2014). Texture Evolution of Commercially Pure Copper during Ultra-Thin Strip Rolling. *Advanced Materials Research*, 941-944, 1532–1536. doi:10.4028/www.scientific.net/amr.941-944.1532
33. Semenov, A.B., Fomina, O.N., Muranov, A.N., Kutsbakh, A.A. and Semenov, B.I. (2019a). The modern market of blank productions in mechanical engineering and the problem of standardization of new materials and technological processes. *Advanced Materials and Technologies, 1*, 3-11. doi: 10.17277/amt.2019.01.pp.003-011
34. Semenov, A.B., Kutsbakh, A.A., Muranov, A.N. and Semenov, B.I. (2019b). Metallurgy of thixotropic materials: the experience of organizing the processing of structural materials in engineering Thixo and MIM methods. *IOP Conference Series: Materials Science and Engineering, 683*, 012056. doi:10.1088/1757-899x/683/1/012056
35. Strycharska, D. (2019). Analysis of roll wear costs during multi-strand rolling of

ribbed bars using new slitting pass system. *New Trends in Production Engineering, 2*(2), 267-278. doi:10.2478/ntpe-2019-0091

36. Wang, S., Cheng, S., Yu, H., Rao, Z., and Liu, Z. (2013). Experimental investigation of Al–Cu composed tube–fin heat exchangers for air conditioner. *Experimental Thermal and Fluid Science*, 51, 264–270. doi: 10.1016/j.expthermflusci.2013.08.007

37. Yakovleva, I.L., Kar'kina, L.E. and Zubkova, T.A. (2011). Effect of cold plastic deformation on the structure of granular pearlite in carbon steels. *The Physics of Metals and Metallography, 112*(1), 101-108. doi:10.1134/s0031918x11010388

38. Yoshimi, T., Matsumoto, S., Tozaki, Y., Yoshida, T., Sonobe, H. and Nishide, T. (2009). Work hardening and change in contact condition of rolling contact surface with plastic deformation. *Tribology Online, 4*(1), 1-5. doi:10.2474/trol.4.1

39. Zhang, P., Kou, S., Lin, B., and Wang, Y. (2014). Optimization for radial knurling connection process of assembled camshaft using response surface method. *The International Journal of Advanced Manufacturing Technology*, 77(1-4), 653–661. doi:10.1007/s00170-014-6486-z

40. Zheng, D. (2014, 10-11 July). *Industrial engineering and manufacturing technology.* Paper presented at the International Conference on Industrial Engineering and Manufacturing Technology. doi:10.1201/b18144

$$L'_{CON1} = \frac{\pi r\left(\varepsilon_1+\varepsilon_2\right)}{180°} + \frac{2H\left(1-2/n\right) - S\mathrm{tg}\alpha - 4r\left[1-\sin\left(\varepsilon_1/2\right)\right]}{2\cos\left(\varepsilon_1/2\right)} + \frac{2H\left(1-2/n\right) + S\mathrm{tg}\alpha + 4r\left[1-\sin\left(\varepsilon_2/2\right)\right]}{2\cos\left(\varepsilon_2/2\right)} \quad \text{(Eq. 33b)}$$

$$\eta_{CON} = \frac{\pi r\left(\varepsilon_1+\varepsilon_2\right)\cos\left(\alpha/S\right)}{180°} + \psi;$$

$$\psi = \frac{\cos\alpha}{2S}\left[\frac{2H\left(1-2/n\right) - S\mathrm{tg}\alpha - 4r\left[1-\sin\left(\varepsilon_1/2\right)\right]}{\cos\left(\varepsilon_1/2\right)} + \frac{2H\left(1-2/n\right) + S\mathrm{tg}\alpha + 4r\left(1-\sin\left(\varepsilon_2/2\right)\right)}{\cos\left(\varepsilon_2/2\right)}\right] \quad \text{(Eq. 35)}$$

Figure 1. *Finned tube heat exchanger*

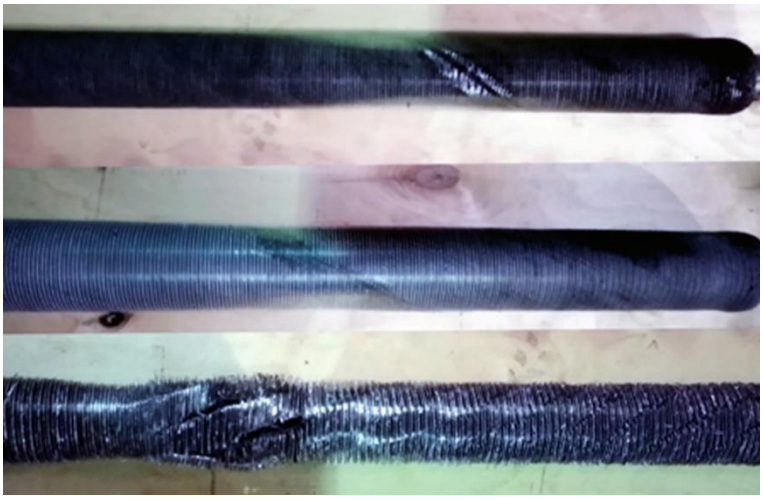

Figure 2. *Possible unacceptable defects at cold knurling*

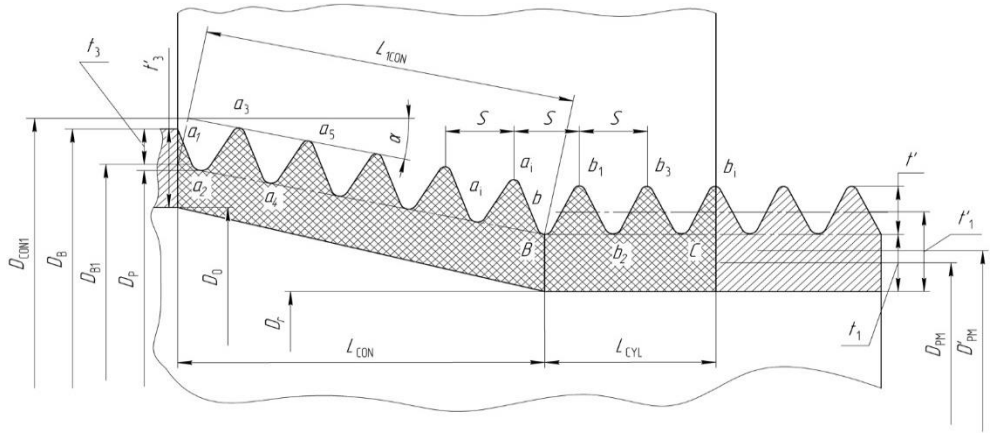

Figure 3. *Frontal section of the deformation zone and projection of the contact surface*

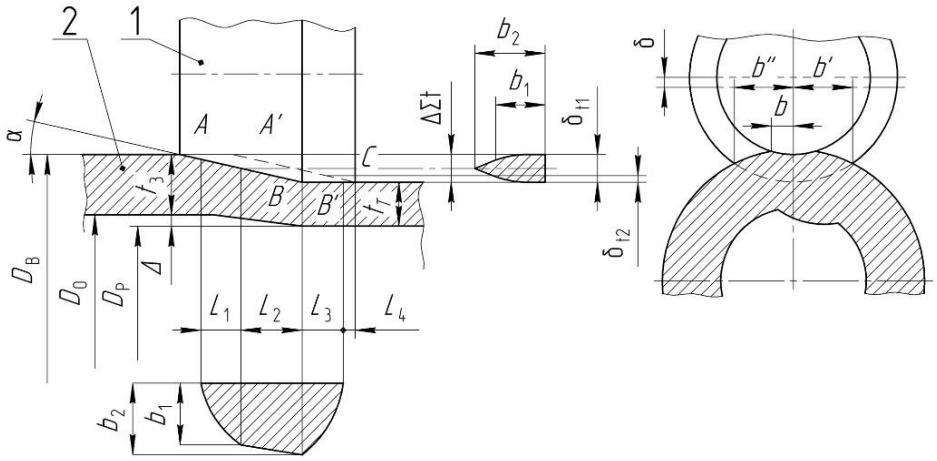

Figure 4. *Frontal and profile sections of the deformation zone and projection of the contact surface: 1 - knurl; 2 - ring blank*

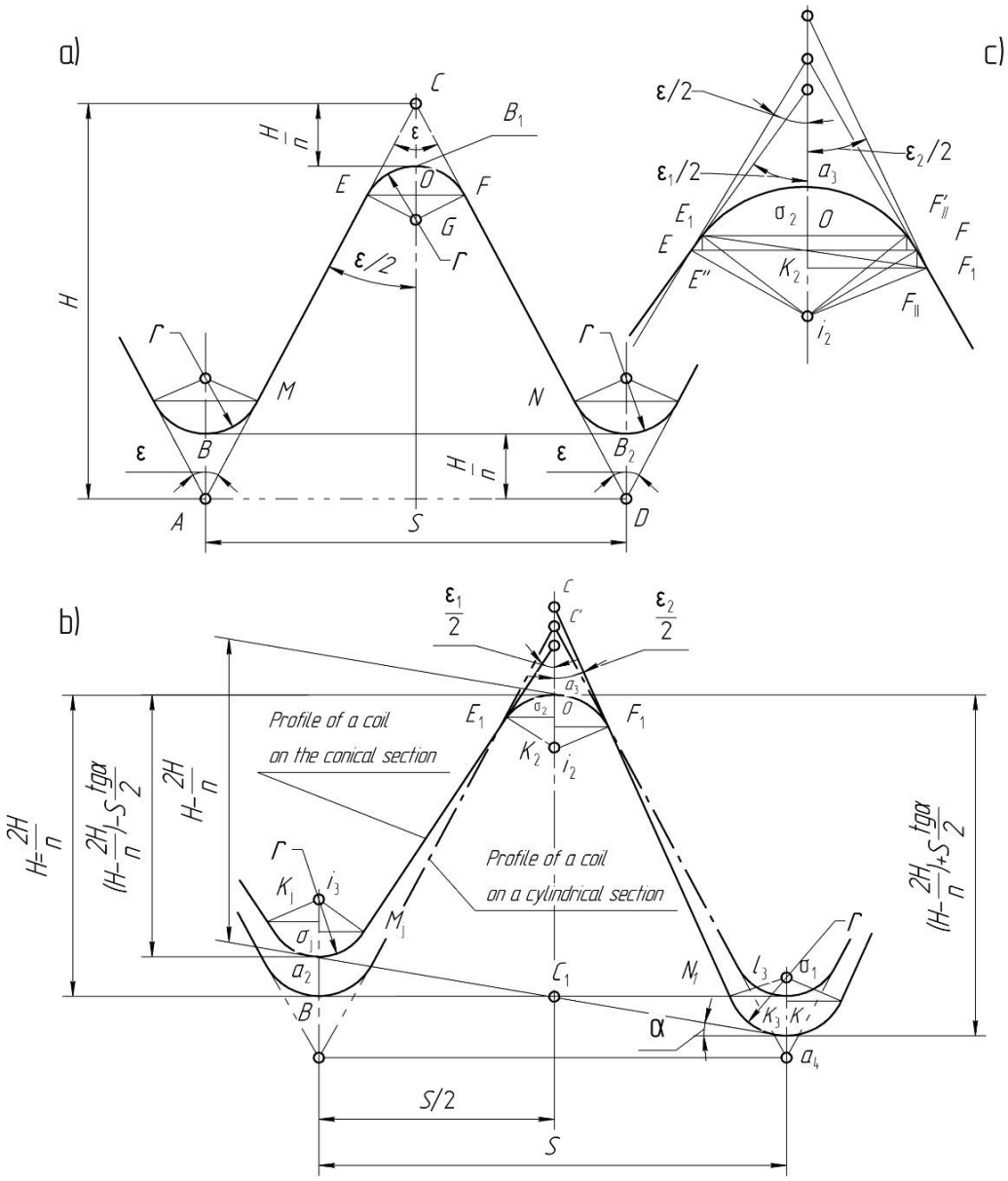

Figure 5. *Profile of a turn of a ring-cut knurl: a) in a cylindrical section; b), c) - on the cylindrical and conical sections (diagrams of the relations of the geometric dimensions of the profile of the turn)*

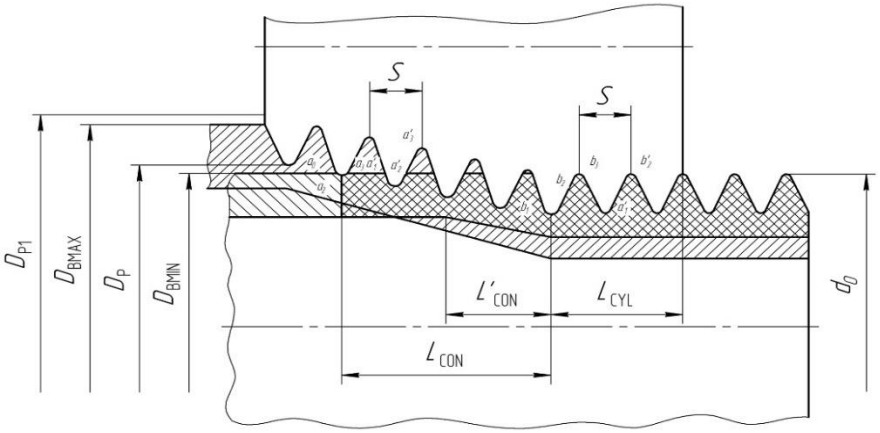

Figure 6. *Dimensions of the deformation zone depending on the billet's diameter*

8. APPENDIX:

THE LEGEND OF ABBREVIATIONS:

b_X – the width of the contact surface;

b_1 – deformation zone width at the border of the 1st section;

b_2 – deformation zone width at the border of the 2nd section;

d – engagement diameter of the finned surface;

d_1 – inner diameter of the finned surface along with the dents;

d'_{0MIN} – minimum outer diameter of the finned surface;

d'_{0MAX} – maximum outer diameter of the finned surface;

D – the knurl's engagement diameter;

D_1 – the knurl's outer diameter;

D_{BM} – the mean diameter of a billet to be knurled;

D_{BMAX} – maximum diameter of a billet to be knurled;

D'_{BM} – the mean diameter of a ring blank;

D'_{BMIN} – minimum outer diameter of a blank pipe to be knurled;

D'_{BMAX} – maximum outer diameter of a blank pipe to be knurled;

D_H – outer diameter of the finned surface along with the vertices;

D_{PM} – the mean diameter of a knurled part;

D'_{PM} – the mean diameter of a knurled finned part;

D_{CON1} – nominal mouth diameter of the conical portion of the tool along with the dents;

F_C – contact area at knurling;

F_{HOR}– horizontal plan of the billet metal contact surface with the knurl;

F_{VERT}– vertical plan of the billet metal contact surface with the knurl;

H – theoretical height of the initial triangular profile of the forming tool;

L – the total length of the smooth knurl's contact surface and the ring blank;

L_1 – the length of the smooth knurl's contact with the ring blank at the *AA'* section;

L_2 – the length of the smooth knurl's contact with the ring blank at the *A'B* section;

L_3 – the length of the smooth knurl's contact with the ring blank at the *BB'* section;

L – total length of the pipe billet and the ring-cut knurl;

L'_i – length of the pipe billet's contact surface and the ring-cut knurl;

L_{1CON} – the length of the straight conical section along with the apices of the forming tool;

L_{CYL} – the length of the cylindrical part of the knurl along with the apices of the forming tool;

L'_{1CON} – the length of the actual contact finned surface along with the knurl's taper lead;

L'_{CYL} – the actual length of the contact finned surface along with the cylindrical part of the knurl;

n_{CON} – the number of turns of the conical section;

n_{CYL} – the number of turns at the cylindrical (calibrating) part of the tool;

P_{ROL} – the knurling force;

r – the rounding radius at the finning apices at the processing knurl;

S_Z – spacing equal to the length of the L_1 section of the contact surface of the smooth roller and the ring blank;

S – fin spacing at the processing knurl;

t_i – finning height;

t_B – the wall thickness of the billet;

t_P – minimum wall thickness of the billet;

z – the amount of knurls in the processing head;

Δt_Σ – the difference between t_B and t_P;

Δ – half of the difference between D_0 and D_P;

δt_X – reduction;

α – the angle between the billet's axis and billet's forming surface contacting the knurl;

ε – the pressure angle at the apex of the initially finning triangle at the process tool;

ξ – the engagement coefficient depending on the finning characteristics;

η_{CON} – the proportionality coefficient, considering the excess length of the contact surface for the conical part of the knurl;

η_{CYL} – the proportionality coefficient, considering the excess length of the contact surface for the cylindrical part of the knurl;

μ_{Σ} – total rolling-out of the pipe billet in longitudinal section;

μ'_{Σ} – total rolling-out of ring blank in the longitudinal direction at knurling finning by the ring-cut knurls;

ρ – specific pressing forces at knurling.